

# Shape Classification Using Contour Simplification and Tangent Function

Chi-Man Pun and Cong Lin

**Abstract**— In this paper we propose a new approach for image classification by simplifying contour of shape and making use of the tangent function as image feature. We firstly extract shapes from a sample image and connecting pixels of its contour. The extracted contour is simplified by our algorithm and converted into tangent function which is regarded as a feature. The tangent function represented a shape is input into classified system and compared with tangent function from existed classes by computing their distance. The input sample image will finally be classified into a class that has minimum distance with it. The experimental results show the proposed method can achieve high accuracy.

**Keywords**— Shape classification, contour, simplification, tangent function.

## I. INTRODUCTION

Classifying a group of images, telling out which class they belong to, is an important problem in shape classification and image retrieval systems. Shape classification systems are generally used in applications like image databases in which the shape segmented from an image will be classified into a class that have exit in database according to a defined criterion, which judge how similar or dissimilar the sample shape to those existed in classes. Often the criterion, or called metric, is features based. Simply comparison of pixels does not work well on most systems, since the difference between images is reflected on differences of certain features. Shape is an important visual feature of an image for content-based image retrieval or recognition [1]. Techniques for shape feature extraction can be generally classified into two categories: boundary-based methods and region-based methods. Boundary-based methods are widely used. They depend so much on the boundary that a slight change can cause grave retrieve errors. Compared with boundary-based ones, region-based techniques are comparatively more suitable for general applications. Zernike Moments (ZM) method is one of the most desirable region-based methods. The modified ZM has been adopted by MPEG-7 as a standard region-based descriptor. The generic Fourier Descriptor is another favorable method proposed in recent years. However, most of

the existing methods cannot achieve high recognition rate for images with complex inner shapes. Therefore, researches in the field of similarity measuring and image matching mainly focus on image features nowadays[1, 2]. For example, in[3], Inner-Distance was used as an feature of shape that described the characteristics unique from others and in[4] Radon Composite Features was employed. One widely used approach is template matching. However, a direct template matching also has its main disadvantage: very high computational cost. This is owing that representation of template from image can be complex in processing, for instance, the higher resolution or more noise, the heavier computation is required. A meaningful similarity measuring should have two important elements: finding a set of features that adequately contain characteristics that can be employed to differentiate images and endowing the feature space with a proper metric.[2] Researchers have also done substantial studies on that how to choose features for a particular problem [5, 6]. On the other hand, designing a proper metric is equally important. Most of the time, a metric is designed for a specific features. Mathematicians have established the reasonable architecture for a metric, defining a metric as a cost function  $d(\bullet, \bullet)$ [7] satisfying conditions:

- 1)  $d(A, B) \geq 0$  for all A and B.
- 2)  $d(A, B) = 0$  if and only if  $A=B$ . And  $d(A, A)=0$  in particular a shape resembles itself.
- 3)  $d(A, B) = d(B, A)$  for all A and B.(Symmetry)
- 4)  $d(A, B) + d(B, C) \geq d(A, C)$  for all A, B and C. (Triangle Inequality)

Moreover, a mature Shape classification system is also required to be invariant under transition, rotation, and change of scale.

This paper presented an approach to obtain an approximation of shape contour and proposed a novel approach to classify shapes into multiple classes based on the tangent function.

The procedure of our system is given as following:

This work was supported in part by the Research Committee of University of Macau under the Grant: RG056/08-09S/PCM/FST.

C.-M. Pun and Cong Lin are with the Department of Computer and Information Science, University of Macau, Macau S.A.R., China. (e-mail: {cmpun, ma865551}@umac.mo).

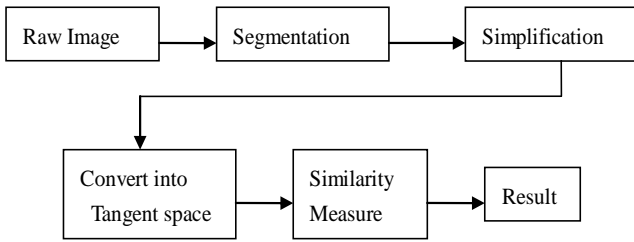


Fig. 1 The process of the proposed approach

The raw images are input into to a segmentation system. The system extracts and segments the shape of objects by color, hue or even contrast etc. Extensive literature and approaches concerning shape segmentation are available.[1, 8] Since the standard dataset for image retrieval are simple shapes with blank background and considering this paper mainly focuses on shape rather than segmentation, we supposed shapes have already segmented from images. Here are working steps in details:

S1. Extract shapes from a sample image and connecting pixels of its contour.

S2. The simplification is imposed on the shapes firstly. The output is a simplified, de-noised, and more linear boundary and of less pixels which preserves important and relevant shape information of the original image. The remaining points constitute significant part of the shape. This step also reduces computational complexity for following steps.

S3. Every two consecutive points are viewed as a line segment or vector. The simplified shape is converted into tangent space and angles of every two consecutive vectors are mapped to the range of tangent function.

S4. The array of values of Tangent function is then input into classification system. The system compares the tangent function from sample with those typical tangent functions in each class. And finally find out a class that has minimum distance with the sample.

We will give more details in section II in this paper concerning contour simplification. The details of definition and usage of tangent function will be provided in section III. In section IV, a procedure for a novel image classification system is given and explained in details. An analysis on result and discussion is presented in section V. Finally, a summary concluded this approach in the last section.

## II. CONTOUR SIMPLIFICATION

Generally, a segmented shape contains some noise or small dents which contribute little to its features and decelerate the process of measuring. In psychology, there are strong evidence that concludes recognition from human vision

mainly relies on significant parts of shape.[9] Therefore, the noise and insignificant information on the boundary should be removed and those significant points on the large turning corners should be remained. A simplification process is necessary before measuring in order to obtain a simpler shape that preserves the significant shape features. Another benefit of simplification is to reduce data storage and therefore accelerate processing in later stage. The simplification process is also called discrete Curve Evolution Procedure[10, 11]. The basic idea of simplification is: we replace two consecutive line segments on the contour with a single line segment joining their endpoints, if joint 'condition' of two consecutive line segments lower than a pre-defined threshold. The joint 'condition' is a function which is defined to compute the significance of the two consecutive line segments and their angle contributed to the whole shape. And our approach reduces every shape to a fixed number of points. To achieve this, we first define the relevance function  $K(s_1, s_2)$ [10, 11]:

$$K(s_1, s_2) = \frac{\beta(s_1, s_2) \cdot L(s_1) \cdot L(s_2)}{L(s_1) + L(s_2)} \quad (1)$$

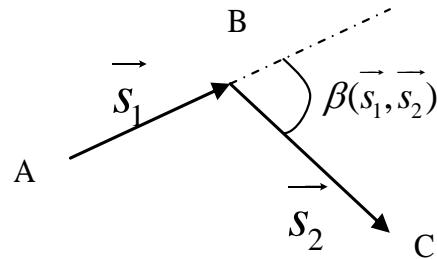


Fig. 2 Turn angle  $K(s_1, s_2)$  between two vectors

The relevance function  $K(s_1, s_2)$  is defined on two consecutive vectors and indicates how much significance the triangle consist of  $s_1$  and  $s_2$  contributes to the whole shape. The higher value of  $K(s_1, s_2)$ , the more significance of the two consecutive vectors contribute to the shape. If there is an  $i$ , such that the  $K(s_i, s_{i+1})$  is minimum and points of the shape are still more than the pre-defined constant, the two vectors are to be replaced by one that connects the endpoints. This operation iteratively traverses the shape boundary until number of points is reduced to our pre-defined value. From the definition of  $K(s_1, s_2)$ , we can see that the larger angle and longer line segments gives a higher function value so that a more significant part will not be replaced.

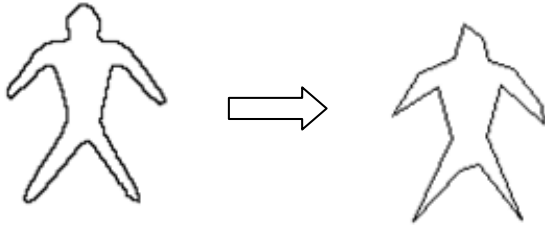


Fig. 3 An image boundary to corresponding simplified one

From the figure, after simplification, the result generated a simplified shape which is more linear and of less noise and preserved shape information as well. Note that data of original shape is array of locations of neighboring points, while data of simplified one is array of discrete points in clockwise orientation.

### III. TANGENT FUNCTION

A tangent function is a representation of a shape  $C$  and interpreted as a polygonal curve with all vertices without loss of information. And reconstruction of the original shape is reversible if the position of one vertex is noted down in advance. A vector on boundary is mapped to a value and the whole shape is mapped into a step function which can be viewed as a signal and analyzed by other tools, e.g. stationary wavelet. In [7, 8], tangent function is defined as a step function. Let  $C$  be a polygonal curve. It is defined as a function on  $C: [0,1] \rightarrow \mathbb{R}^2$ , the length of  $C$  is rescaled to 1 in order to normalize the shape so that the similarity measure between two shapes can be invariant under scale-of-change.

The tangent function is also called a turning function which is a multi-valued function  $T(C): [0,1] \rightarrow [-\pi, \pi]$  defined by  $T(C)(s) = C'_-(s)$  and  $T(C)(s) = C'_+(s)$ , where  $T(C)(s) = C'_-(s)$  and  $T(C)(s) = C'_+(s)$  are left and right derivatives of  $C$ . The value of  $T(p)$ ,  $p$  is a point on  $C$ , is angle between a reference vector and the line segment vector which  $p$  lay on.

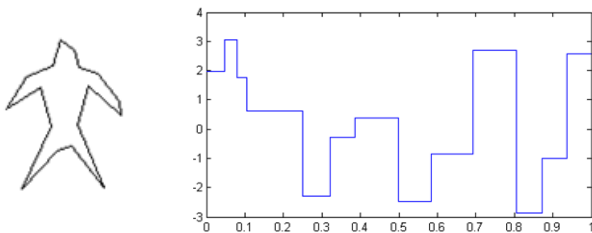


Fig. 4 A simplified boundary and its tangent function

The tangent function  $T(C)(s)$  traces where the turning takes place on the contour, increasing with left turns and decreasing with right turns, makes it a feature frequently used as a shape signature. [7, 12-15] In order to achieve rotation invariant, we would like to modify and improve the original tangent function. In our version, on one hand, we pick up the

farthest pixel from centroid in the shape to start simplification; on the other hand, the value of tangent function corresponding to x-axis is the relative angle change to current vector to previous one (from the graph of step function, that means the value of current step is assigned by the difference that value of current step minus value of previous step). In this case, the scale of y-axis represents the change of direction from previous line segment.

### IV. SHAPE CLASSIFICATION

In classification system, some templates should be stored in the system in advance and samples are input into the system then compared with each template to determine which class it belongs to. In our idea, templates are preprocessed and stored in the form of tangent functions. Each class may include several templates that shares some part features but with different visual shapes. In order to compare templates and samples, the system extracts the boundary of samples, simplifies the boundary and converts it into a form of tangent function. The similarity metric is defined as follows[7]:

$$D(A, B) = \int_0^1 |T_A(s) - T_B(s)|^p ds \quad (2)$$

The degree of similarity between two shapes  $A$  and  $B$  is measured by calculating the metrical distance between two tangent functions.

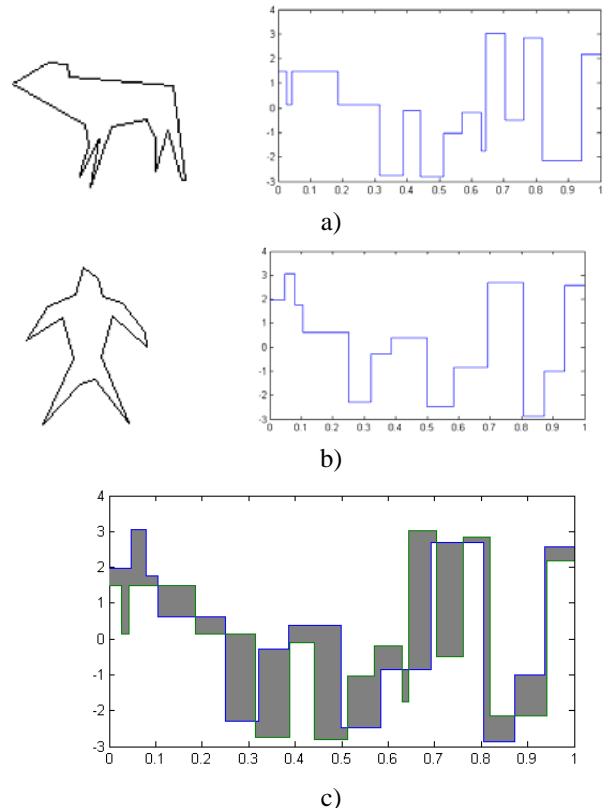


Fig. 5 c) the area between two tangent functions

In Fig. 5, the area in gray is the distance between two tangent functions. Similar tangent functions generate smaller

distance. Therefore, classification can be done by comparing the template from the sample with each template of each class and finding out that one which has minimal distance with the sample template. And finally, the shape will be classified into the class which the minimal distance template belongs to.

We also present our procedure in pseudo-code as follows:

*INPUT* Sample set:  $S = \{s_1, s_2, \dots, s_n\}$ ;

Class set:  $C = \{C_1, C_2, \dots, C_m\}$ ;

A Class with several templates included:  $C_j = \{t_{j1}, t_{j2}, \dots\}$

*PROCEDURE*

For  $i=1$  to  $n$

Segment Shape and extract boundary from  $s_i$

Simplified the original boundary

Generate tangent function  $T(s_i)$  from simplified

boundary

For  $j=1$  to  $m$

For  $k=1$  to the size of  $(C_j)$

Compute distance  $D(T(s_i), t_{jk})$

Note down the Class index of minimal D: Min

End

End

Sample is classified into  $C_{Min}$

End

## V. EXPERIMENTAL RESULTS

An experiment for evaluating this approach is performed on a widely used dataset provided by [16]. There are in total 99 samples in the dataset which belongs to 9 classes. Each class contains 11 samples with relatively similar forms but influenced by occlusion, rotation, articulation and missing parts. And this dataset is used as templates. Other datasets with scaled rotated variations are generated from the original templates and used as samples.



Fig. 6. Image dataset of 99 testing shapes provided by Kimia et al [16]

In our experiment, we generated 16 sample datasets base on the original one. They are rotated 0, 30, 45 and 90 degree and scaled 2/3, 1, 4/3 and 2 times respectively. The overall results are showed as follows. All the shapes are simplified into fixed 28 points.

TABLE I. Overall correctly classification rates for each sample dataset

Scaled Rotated	2/3	1	4/3	2
0°	97.0%	100.0%	100.0%	100.0%
30°	86.9%	85.9%	83.8%	84.9%
45°	85.9%	85.9%	83.8%	85.9%
90°	97.0%	100.0%	100.0%	100.0%
180°	96.0%	99.0%	99.0%	99.0%

From table I, we can see that the performance is quite insensitive to change of scale. Even in the worst cases when all samples are scaled to 2/3, there are only 3 samples in a sample set misclassified. This is mainly because, after the simplification, the length of boundary is normalized and all of the resized samples are compared in the same scale. However, we found that rotation of samples affects the performance of this approach significantly when samples are not rotated with 90\*n degree and it can be attributed to change of noise on the boundary, since rotation with 90 degree will not change relative position of points on boundary otherwise noise may be added and the relative position can be changed. Although rotation and slight change on boundary might affect tangent function, tangent functions from the same category maintain relatively similar forms. First column in Table 1 is the worse cases. A further investigation is to find out classification rates for each class.

TABLE II Classification rates in each class

Rotated Class	30°	45°	60°
Quadrupeds	9	9	10
Humans	11	11	11
Airplanes	9	9	7
Grebes	8	10	7
Fish	9	10	10
Hands	11	8	8
Rays	11	11	11
Rabbits	8	9	8
Wrenches	10	8	10
Overall	86.90%	85.90%	82.80%

Form Table II, the experiment successfully classified all samples in category Humans and Rays and obtain high correct rate in category Fish. Samples in these categories generally have smooth boundary and sharp turns.

### Comparison with Composite Features by Radon Transform

In mathematics the radon transform in two dimensions, named after the Austrian mathematician Johann Radon, is the

integral transform consisting of the integral of a function over straight lines  $\lambda = x \cos \theta + y \sin \theta$  (1). Radon transform can be represented by

$$R(\lambda, \theta) = \int_{-\infty}^{\infty} \int_{-\infty}^{\infty} f(x, y) \delta(\lambda - x \cos \theta - y \sin \theta) dx dy \quad (3)$$

When a generalized image is represented by a function  $f(x, y)$ , the radon transform is used to calculate the projection of the image intensity along a radial line oriented at a specific angle  $\theta$ . In image processing phase, the general image function  $f(x, y)$  is replaced by binary discrete signal  $S_D(x, y)$  with the size  $m$  by  $n$ , where

$$S_D(x, y) = \begin{cases} 1, & \text{if } (x, y) \in D \\ 0, & \text{otherwise.} \end{cases}$$

The density distribution along lines as Formula (1) can be represented by

$$D_S(\lambda, \theta) = \sum_{y=1}^n \sum_{x=1}^m S_D(x, y) \delta(\lambda - x \cos \theta - y \sin \theta) \quad (4)$$

Where  $\theta$  represents the line direction and  $\lambda$  is the distance away from the coordinate's origin. Usually, these two parameters  $\theta$  and  $\lambda$  are equidistantly chosen and their numbers are denoted as  $N_\theta$  and  $N_\lambda$ . The number  $D_S$  is a matrix with size  $N_\theta$  by  $N_\lambda$  representing the image density distribution along different lines.

The image density distribution properties of periodicity and symmetry can be easily obtained from the definition,

$$\begin{aligned} D_S(\lambda, \theta) &= D_S(\lambda, \theta + 2k\pi) \\ D_S(\lambda, \theta) &= D_S(-\lambda, \theta \pm (2k + 1)\pi) \end{aligned} \quad (5)$$

Parameter  $\theta$  defaults to 0:179,  $N_\theta$  equals to 180 and  $N_\lambda$  are determined by the size of the image.

#### Radon Invariant Features

For an arbitrary angle  $\theta$ , we denote

$$E_S(\theta_i) = \sum_{\lambda=1}^{N_\lambda} R_S(\lambda, \theta_i) \quad (6)$$

where  $E_S(\theta_i)$  is the energy of Radon Transform along line  $\theta_i$ , and parameter  $N_\lambda$  is the length of Radon Matrix  $R_S$  in  $\lambda$  direction. According to the conservation of energy, we have  $E_S = E_S(\theta_i) = E_S(\theta_j)$  for any given angle.

A shape in the image can be resized. In order to meet the need of size invariant, modified image density distribution along lines  $L(\lambda, \theta)$  is defined by

$$D'_S(\lambda, \theta) = \sqrt{E_0 / E_S} R_S(\sqrt{E_S / E_0} \lambda, \theta) \quad (7)$$

where  $E_0$  is a constant determined by the size of image, and variable  $\sqrt{E_S / E_0}$  is used to make the shape size invariant.

Fig 7 (a) illustrates a series of butterflies. Picture (a) is the original image. The remaining ones in the first column are the geometry transformations of (a). Picture (b) is resized by 0.5 time; (c) is translated by 60 by 0 pixels; (d) is rotated counter-clockwise by 30 degrees. The second column is the image density distribution  $D_S$  of Column One respectively. Label  $x$  is the degree from 0 to 179, and Label  $y$  is the image density distribution in different  $\lambda$  values. The third column is the modified image density distribution  $D'_S$ . Label  $x$  and  $y$  are the same with Column Two. The fourth column is the curve of  $DF'_S(\theta_i)$ .

By compared (a2) and (b2), we can see  $D'_S$  is size invariant while (a1) and (b1) reflect  $D_S$  is not.

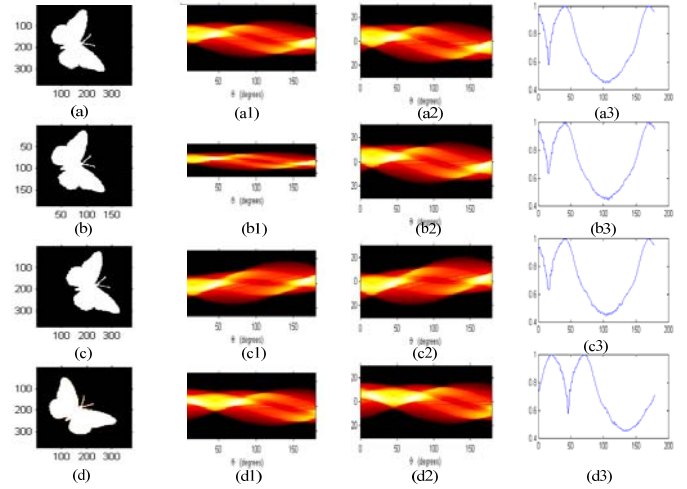


Fig 7: Radon Invariant Features. (a) Original Image; (b) resize 0.5 time of (a); (c) translate 60 by 0 pixels; (d) rotate 30 degrees. (\*1) are image density distributions  $D_S$  for corresponding (\*) pictures. (\*2)  $D'_S$ . (\*3) are curves of feature  $DF'_S(\theta_i)$ .

A shape can be shifted in the image. Luckily the image density distribution along lines  $L(\lambda, \theta)$  is just shifted. The boundary can be easily distinguished by judging the first none zero value in Radon Matrix. Thresholds,  $\min \lambda$  and  $\max \lambda$ , are employed to ascertain the valid range of the shape area along direction  $\theta_i$ .

$$\begin{aligned} \min \lambda &= \min_{\lambda} \{D'_S(\lambda, \theta_i) > D_n\} \\ \max \lambda &= \max_{\lambda} \{D'_S(\lambda, \theta_i) > D_n\} \end{aligned} \quad (8)$$

where  $D_n$  is a threshold controlling the range of shape area along a particular line with angle  $\theta_i$ ; this parameter is used to suppress noise and outliers.

The energy of Radon Transform (6) now changes to

$$E'_S(\theta_i) = \sum_{\lambda=\min \lambda}^{\max \lambda} D'_S(\lambda, \theta_i) \quad (9)$$

Another distribution feature can be calculated by

$$DF'_S(\theta_i) = \sqrt{\sum_{\min \lambda}^{\max \lambda} (D'_S(\lambda, \theta_i) - \frac{E'_S(\theta_i)}{\|\max \lambda - \min \lambda\|})^2} \quad (10)$$

The shape density discrimination can be normalized through

$$DF'_S(\theta_i) = DF'_S(\theta_i) / \max\{DF'_S(\theta_i)\} \quad (11)$$

The last column in Fig. 7 illustrates the shape discrimination  $DF'_S(\theta_i)$ . By comparing the first three ones, the translation and size invariant features can be easily found out. Especially, when images are rotated by 30 degrees, curve  $DF'_S(\theta_i)$  is shifted or rotated by 30 degrees. This characteristic inspires us to find a rotation invariant discrimination, which will be covered in Section 3.

#### THE STATIONARY WAVELET TRANSFORM

Wavelets are mathematical functions that cut up data into different frequency components, and then study each component with a resolution matched to its scale. Classical discrete wavelet transform is not time invariant. In order to restore wavelet transform shift invariance, the stationary wavelet transform (SWT) was employed.

Stationary wavelet transform (SWT) is shift invariant. Fig 8 describes the basic decomposition steps for one-dimensional SWT. The approximation and detail coefficients at level 1 are both of size N, which is the signal length.

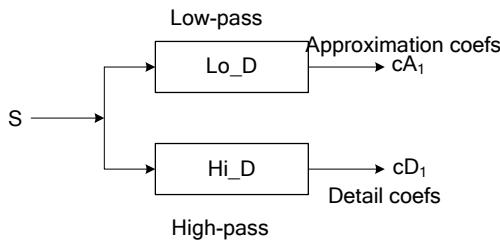


Fig 4: Basic decomposition step for two dimensional signals

After applied the stationary wavelet transform,  $DF'_S(\theta_i)$  can be rotation invariant. Fig 5 (a) and (c) are the exact curves as in Fig. 3 (a3) and (d3), and their corresponding stationary wavelet transforms are shown in Fig 5 (b) and (d). From this figure, the rotation invariant features can be obtained.

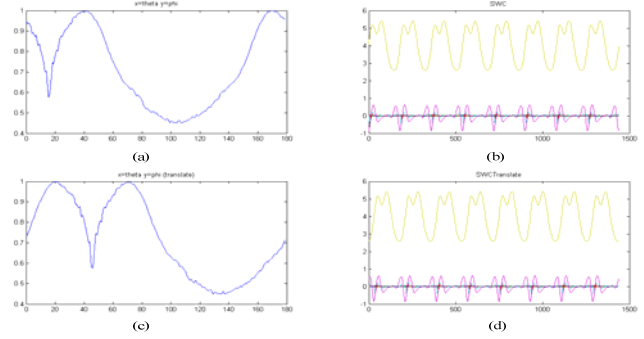


Fig 8: Rotate Invariant Features. (a) The exact curve  $DF'_S(\theta_i)$  as in Fig7 (a3); (b) Level 6 sub-wavelet of (a); (c) the exact curve  $DF'_S(\theta_i)$  as in (b3); (d) Level 6 sub-wavelet of (c).

A modified Radon transform plus a stationary wavelet transform, called Radon Wavelet Composite Descriptor (RWCD), can be used to describe invariant shapes in size, translation and rotation. RWCDs is defined as

$$RWCD_S = swc(DF'_S(\theta), Level, 'wname') \quad (12)$$

where  $\theta \in [0,180)$ , Parameter Level is used to decide the total number of sub-wavelets and RWCD is a matrix with size 180 by Level.

The distance between Shape i and j can be calculated by

$$Distance = \sum_{m=1}^{Level} \sum_{n=1}^{180} \|RWCD_{S,imn} - RWCD_{S,jmn}\| \quad (13)$$

This distance is used to determine the similarity between two shapes. In the experiments phase, it will be adopted to determine the retrieve or recognition results.

Fig 9 selects four different levels 4, 6, 8, and 10. This figure shows that when level K increases, the recognition rates of the nine categories rise. The reason is that when K increases, the number of sub-wavelets rises, and the distance between pictures is calculated in more detail.

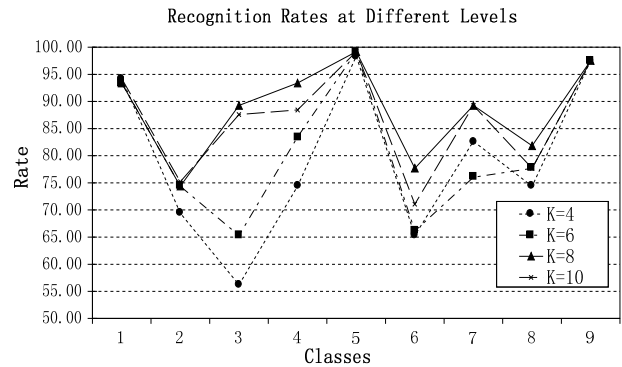


Fig 9: Recognition Rates at Different Levels

#### Shapes with Complex Inner Structure

As a region-based analysis method, RWCD can deal with shapes with complex inner structures. A test shape database is

used here. This database consists of 504 images which are selected from the MPEG-7 (CE-2) region-based database. They are organized into 24 groups, as shown in Fig 10. In each group there are 10 similar shapes including four scaled ones, and five rotated ones. The precision–recall diagrams are presented in Fig 11 by comparing with two classical retrieval methods, Zernike Moments [9] and Generic Fourier Descriptors[10].

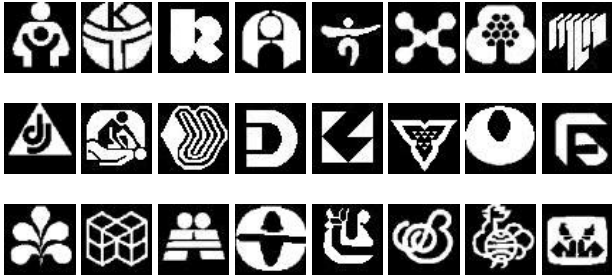


Fig 10: Shape database selected from the MPEG-7 (CE-2)

Fig 11 reflects that the more detail the images is, the higher recognition rate is. In order to raise the recognition rate, the size of the original images can be increased.

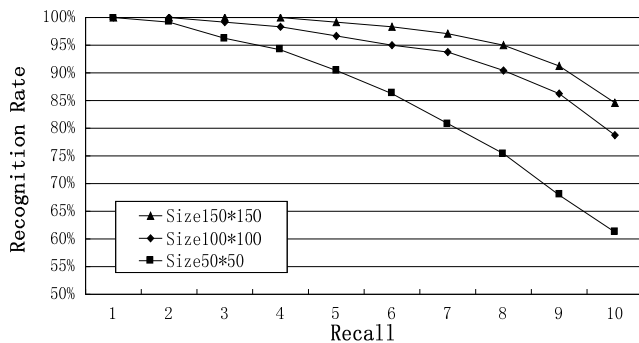


Fig 11: Recognition Rates to Images with Different Size

Fig 12 reflects the ability of each method in describing shapes with complex structures and the overall robustness under various geometric transforms. It can be observed that the proposed RWCD method can handle shapes with complex inner structures more effectively.

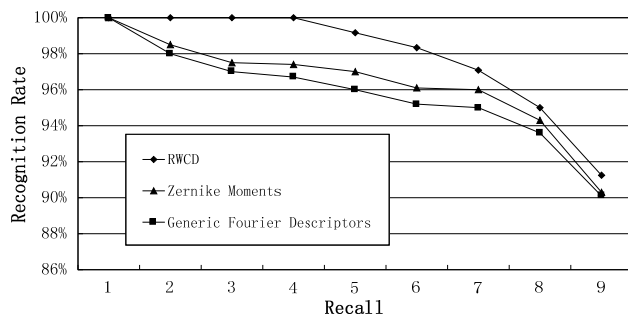


Fig 12: Recognition Rates of Different Retrieval Methods.

## VI. CONCLUSION

In this paper, we proved that tangent function can be applied on classification system and our experiment result turned out to be reasonably good. However, we also found that changes of noise on the contour affect the tangent functions generated from images. That may lead to different tangent functions from same shape with different degrees rotated. For instance, B is a rotated shape from A. They may have different tangent functions. And distance between A and B may be larger than certain neighbor shape of B. Fortunately; even if minimum distance is from another shape from the same category, we found most shapes maintain very small distance when rotated, while have large distance with shapes in other categories.

## REFERENCES

- [1] R. E. w. Rafael C. Gonzalez, *Digital Image Processing*, Englewood Cliffs, N.J.: Prentice Hall, 2008.
- [2] M. Simone Santini, IEEE, and Ramesh Jain Fellow, IEEE, "Similarity Measures," *IEEE TRANSACTIONS ON PATTERN ANALYSIS AND MACHINE INTELLIGENCE*, vol. 21, no. 9, pp. 871-882, 1999.
- [3] L. Haibin, and D. W. Jacobs, "Shape Classification Using the Inner-Distance," *Pattern Analysis and Machine Intelligence, IEEE Transactions on*, vol. 29, no. 2, pp. 286-299, 2007.
- [4] Y. Q. C. Yun Wen Chen, "Invariant Description and Retrieval of Planar Shapes Using Radon Composite Features," *IEEE Trans. Sign. Proc.*, vol. 56, no. 10, pp. 4762-4771, October, 2008.
- [5] R. K. R.Jain, and B. Shunk, *Machine Vision*: McGraw-Hill, 1995.
- [6] A. K. Jain, *Fundamental of Digital Image Processing*, Englewood Cliffs, N.J.: Prentice Hall, 1989.
- [7] L. P. C. Esther M. Arkin, Daniel P. Huttenlocher, Klara Kedem, and Joseph S. B. Mitchell, "An Efficiently Computable Metric for Comparing Polygonal Shapes," *IEEE TRANSACTIONS ON PATTERN ANALYSIS AND MACHINE INTELLIGENCE*, vol. 13, no. 3, pp. 209-215, March 1991.
- [8] S. Xu, "Robust traffic sign shape recognition using geometric matching," *IET Intelligent Transport Systems*, vol. 3, no. 1, pp. 10-18, 2008.
- [9] K. t. K. siddiqi, and B.B.Kimia, "Parts of visual form: Ecological and psychophysical aspects," *Proc. of the IAPR's International Workshop on Visual Form, Capri*, 1994.
- [10] L. J. L. a. R. Lakämper, "Convexity Rule for Shape Decomposition Based on Discrete Contour Evolution," *Computer Vision and Image Understanding*, vol. 73, no. No.3 March, pp. 441-454, 1999.
- [11] L. J. L. a. R. Lakämper, "Shape similarity Measure Based on Correspondence of Visual Parts," *IEEE TRANSACTIONS ON PATTERN ANALYSIS AND MACHINE INTELLIGENCE*, vol. 22, no. 10, pp. 1185-1120, 2000.
- [12] J. H. a. X. Tan, "The similarity between shapes under affine transformation," *Proc. Second Int. Conf. Computer Vision*, pp. 489-493, 1988.
- [13] J. h. a. H. J. Wolfson, "And improved model-base matching method using footprints," *Proc. Ninth Int. Conf. Pattern Recognition, Rome, Italy*, vol. Nov. 14-18, 1988.
- [14] J.T. Schwartz and M. Sharir, "Some remarks on robot vision," *New York Univ., Courant Inst. Math. Sci., Tech. Rep. 119*, vol. Robotics, no. Rep. 25, Apr, 1984.

- [15] H. Wolfson, "On curve matching," *Proc. IEEE workshop Computer Vision, Miami Beach, FL*, No.30-Dec.2, 1987.
- [16] J. C. Daniel Sharvit, H. Teck, and Benjamin B. Kimia, "Symmetry-Based Indexing of Image Databases," *JOURNAL OF VISUAL COMMUNICATION AND IMAGE REPRESENTATION*, vol. 9, no. 4, pp. 366-380, 1998.

**Chi-Man Pun** received the B.Sc. and M.Sc. degrees from the University of Macau in 1995 and 1998 respectively, and Ph.D. degree in Computer Science and Engineering from the Chinese University of Hong Kong in 2002. He currently is an associate professor at the Department of Computer and Information Science of the University of Macau. His research interests include Content-Based Image Indexing and Retrieval, Digital Watermarking, Pattern Recognition, and Computer Vision.